

Dynamic Stress around Two Interacting Cylindrical Nano-Inhomogeneities with Surface/Interface Effects

Le-Le Zhang¹, Xue-Qian Fang¹, Jin-Xi Liu¹ and Ji-Hong Ma¹

Abstract: On the basis of continuum surface elasticity, two interacting cylindrical nano-inhomogeneities with surface/interface effect in a small-sized solid under anti-plane shear waves are investigated, and the dynamic stress around the nano-inhomogeneities is analyzed. The wave function expansion method is used to express the wave field around the two nano-inhomogeneities. The total wave field is obtained by the addition theorem for cylindrical wave function. Through analysis, it is found that the distance between the two nano-inhomogeneities shows great effect on the dynamic stress in nano composites. The effect of the distance is also related to the properties of the nano-inhomogeneities and the interface, the wave frequency, and the incident angle of shear waves. To show the accuracy of the results for certain given parameters, comparison with the existing results is also given.

Keywords: Nano composites; Cylindrical nano-inhomogeneity; Surface/interface stress; Multiple scattering of elastic waves

1 Introduction

To meet the demand for miniaturization in various industries, nano composites are arguably the most actively and extensively developing research areas since the beginning of this century. In recent years, theoretical analysis and experimental investigations on nano composites are attracting more attentions owing to their unique mechanical and physical properties.

Compared with the conventional engineering materials, one distinct characteristic of nano-scale composites is the size-dependent mechanical behavior, which is believed to root in their interface effects. In classical continuum mechanics, the surface is limited to only a few atomic or molecular layers. Thus, if the size of the element is large enough, it is perfectly acceptable to neglect the surface region

¹ Department of Engineering Mechanics, Shijiazhuang Tiedao University, Shijiazhuang, 050043, P.R. China

and to use the bulk parameters of a structural element as its overall parameters. However, when the characteristic sizes of materials and devices shrink to microns or nanometers, surfaces or interfaces may have significant effects on the physical and mechanical properties of solids due to the appreciable ratio of surface/interface area to the volume of matrix. In addition, the neighborhood of the boundary between dissimilar materials in solids may have local material properties different from those of the bulk material on either side (Cheng, et al., 2009). To accommodate this effect in the theory of linear elasticity, a generic and mathematical expression has been presented by Gurtin and his co-workers (Gurtin and Murdoch, 1975; Gurtin et al., 1998). In the following years, several other researchers have contributed to further development of the surface stress theory (e.g., Cahn and Larché, 1982; Cammarata, 1994; Nix and Gao, 1998; Duan et al., 2005).

In the past, most investigations focused on the surface/interface effect under static loadings (Li et al., 2005; Sharma et al., 2003; Sharma and Ganti, 2002). Due to the increasing demand of an understanding of dynamic processes in nanocomposites, it is highly desirable to study the stress in a fully dynamic framework. Very recently, Wu and Dzenis (2006) developed the modified Euler-Bernoulli and Rayleigh-Love rod equations and Timoshenko beam equation to account the surface effects on the longitudinal and flexural wave propagation in straight nanofibers or nanowires. Recently, the scattering of anti-plane shear waves resulting from an elliptical nano-inhomogeneity was also presented (Fang et al., 2010).

This study is to extend the work in (Fang et al., 2010) to the case of two cylindrical nano-inhomogeneities under an oblique incident wave, and the interaction between the two nano-inhomogeneities is considered. The wave fields are expanded by employing wave functions expansion method, and the expanded mode coefficients are obtained by satisfying the boundary conditions of the two nano-inhomogeneities. The addition theorem for cylindrical Bessel function is used to accomplish the superposition of wave fields in nano composites. The numerical solutions of the dynamic stress concentration factor are graphically illustrated. The effects of the incident wave frequency, the material properties of inhomogeneities and interface, and the position of nano-inhomogeneities on the dynamic stress concentration factors in the matrix material are analyzed.

2 Problem formulation

As shown in Fig. 1, an isotropic small-sized material containing two arbitrarily located, cylindrical, elastic nano-inhomogeneities is considered. The radii of the two nano-inhomogeneities are denoted as a_1 and a_2 , respectively. The relative position of the two nano-inhomogeneities is depicted in Fig. 1. For convenience, the polar coordinate systems centered on the nano-inhomogeneities are used. It is

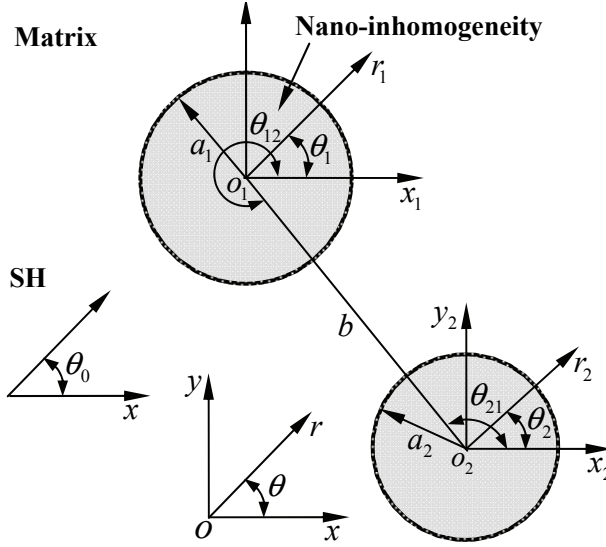


Figure 1: Geometry and coordinate systems of the problem

supposed that the material properties of the two nano-inhomogeneities 1 and 2 are identical. The shear modulus and mass density of the nano-inhomogeneities are denoted by μ_0 and ρ_0 , which are, in general, different from those (μ_m and ρ_m) of the matrix.

In this paper, a coherent interface between the inhomogeneities and the matrix is considered. The surface/interface model developed by Gurtin and Murdoch (1975) is applied. In Gurtin and Murdoch’s model, no slipping of the layer is permitted, and the interface between the nano- inhomogeneities and matrix is modeled as a material surface characterized by the surface tension τ_0 and surface material properties (μ_s and ρ_s).

The dynamic excitation is provided by an anti-plane shear wave with frequency ω , and its incident angle is θ_0 . As the current problem is of anti-plane nature, only the displacement component in the z direction exists. The governing equation in nano composites is expressed as

$$\frac{\partial^2 w}{\partial x^2} + \frac{\partial^2 w}{\partial y^2} = \frac{1}{c^2} \frac{\partial^2 w}{\partial t^2} \tag{1}$$

where $c = \sqrt{\mu_m/\rho_m}$ is the shear wave velocity.

The steady solution of this problem is considered. It is supposed that $w = We^{-i\omega t}$,

then Eq.(1) is rewritten as

$$\nabla^2 W + k^2 W = 0 \tag{2}$$

where $\nabla^2 = \partial^2/\partial x^2 + \partial^2/\partial y^2$ is the two-dimensional Laplacian operator, and $k = \omega/c$ is the wave number of shear waves in the matrix.

3 Wave fields in the nano composites

3.1 Incident wave field

An incident shear wave with incident angle θ_0 propagates in the small-sized composites. For convenience, the incident wave is expanded, in the two local coordinate systems, as (Pao and Mow, 1975)

$$W_1^{(in)} = W_0 \sum_{n=-\infty}^{\infty} i^n J_n(kr_1) e^{in(\theta_1 - \theta_0)} \tag{3}$$

$$W_2^{(in)} = W_0 \sum_{n=-\infty}^{\infty} i^n J_n(kr_2) e^{in(\theta_2 - \theta_0)} \tag{4}$$

where W_0 is the amplitude of incident waves, $J_n(\bullet)$ is the n th Bessel function of the first kind, the superscript (in) denotes the incident waves, and the subscripts 1 and 2 represent the two nano-inhomogeneities, respectively.

3.2 Scattered wave field

Using wave function expansion method, the general solution of scattered field resulting from two nano-inhomogeneities can be expressed, in the two local coordinate systems, as (Pao and Mow, 1975)

$$W_1^{(sc)} = W_0 \sum_{n=-\infty}^{\infty} A_n H_n^{(1)}(kr_1) e^{in\theta_1} \tag{5}$$

$$W_2^{(sc)} = W_0 \sum_{n=-\infty}^{\infty} B_n H_n^{(1)}(kr_2) e^{in\theta_2} \tag{6}$$

where $r_1 = (x_1, y_1)$, $r_2 = (x_2, y_2)$, A_n and B_n are the mode coefficients of scattered waves, and can be determined by satisfying the boundary conditions at the surfaces of the nano-inhomogeneities. $H_n^{(1)}(\cdot)$ is the n th Hankel function of the first kind and denotes the outgoing wave.

3.3 Refracted wave field

The refracted waves, being confined inside the cylindrical nano-inhomogeneities, are standing waves, and represented by

$$W_1^{(r)} = W_0 \sum_{n=-\infty}^{\infty} C_n J_n(k_c r_1) e^{in\theta_1} \quad (7)$$

$$W_2^{(r)} = W_0 \sum_{n=-\infty}^{\infty} D_n J_n(k_c r_2) e^{in\theta_2} \quad (8)$$

where $k_c = \omega / \sqrt{\mu_0 / \rho_0}$ is the wave number inside the nano-inhomogeneities, C_n and D_n are the mode coefficients of the refracted waves, and the cylindrical Bessel functions of the first kind are used to obtain the standing waves.

In Eqs.(7) and (8),

$$k_c = \alpha k, \quad \alpha = \sqrt{\rho / f_0}, \quad \rho = \rho_0 / \rho_m, \quad f_0 = \mu_0 / \mu_m \quad (9)$$

3.4 Total wave field in the matrix material

The total wave field in the nano composites is the superposition of the incident waves and the scattered waves resulting the two nano-inhomogeneities, i.e.,

$$W_1^{(t)} = W_1^{(in)} + W_1^{(sc)} + W_2^{(sc)} \quad (10)$$

$$W_2^{(t)} = W_2^{(in)} + W_2^{(sc)} + W_1^{(sc)} \quad (11)$$

To obtain the total wave field, the scattered wave field in one coordinate system should be transformed into another one. According to addition theorem for cylindrical Bessel function, the following relation can be derived as

$$H_n^{(1)}(kr_2) e^{in\theta_2} = \sum_{m=-\infty}^{\infty} e^{i(m-n)\theta_{21}} H_{m-n}^{(1)}(kb) J_m(kr_1) e^{im\theta_1} \quad (12)$$

Similarly,

$$H_n^{(1)}(kr_1) e^{in\theta_1} = \sum_{m=-\infty}^{\infty} e^{i(m-n)\theta_{12}} H_{m-n}^{(1)}(kb) J_m(kr_2) e^{im\theta_2} \quad (13)$$

It is noted that θ_{21} , θ_{12} and b are shown in Fig.1.

4 Boundary conditions around the two nano inhomogeneities

For the anti-plane shear problem of this study, the boundary conditions at the surface of the nano-inhomogeneity are expressed as

$$W_q^{(t)} = W_q^{(r)} \quad (14)$$

$$\tau_{rzq}^I - \tau_{rzq}^M = \frac{\mu_s - \tau_0}{\mu_m} \frac{\partial \tau_{\theta zq}^M}{\partial \theta_q}, \quad (q = 1, 2) \quad (15)$$

Since the residual surface stress τ_0 always gives rise to an additional deformation field, and is independent of the external loadings, the residual surface stress is ignored in this paper.

The anti-plane shear stresses around the two nano inhomogeneities are expressed as

$$\tau_{rzq}^M = \mu_m \frac{\partial W_q^{(t)}}{\partial r_q}, \quad \tau_{\theta zq}^M = \mu_m \frac{1}{r_q} \frac{\partial W_q^{(t)}}{\partial \theta_q}, \quad \tau_{rzq}^I = \mu_0 \frac{\partial W_q^{(r)}}{\partial r_q}, \quad (q = 1, 2) \quad (16)$$

It is obvious that Eq.(15) contains the intrinsic length parameter $f_s = \mu_s/\mu_m$. For a macroscopic inhomogeneity with a big values of a and $f_s \ll 1$, the surface effects have no effect on the wave fields, and then Eq.(15) reduces to the boundary conditions in classical elasticity. However, when the radius of inhomogeneity shrinks to nanometers, f_s becomes important and the surface effects should be taken into consideration.

5 Solving the scattered and refracted mode coefficients and dynamic stress

By satisfying the boundary condition at the surface of the two nano-inhomogeneities and making use of orthogonality relation of $e^{-is\theta}$, a set of algebraic equations is obtained. After arrangement, the mode coefficients of scattered and refracted waves are determined.

$$A_s H_s^{(1)}(ka_1) + \sum_{n=-\infty}^{\infty} B_n e^{i(s-n)\theta_{21}} H_{s-n}^{(1)}(kb) J_s(ka_1) - C_s J_s(k_c a_1) = -i^s J_s(ka_1) e^{-is\theta_0} \quad (17)$$

$$A_s \left\{ f_s s^2 H_s^{(1)}(ka_1) - \left[s H_s^{(1)}(ka_1) - ka_1 H_{s+1}^{(1)}(ka_1) \right] \right\} \\ + \sum_{n=-\infty}^{\infty} B_n e^{i(s-n)\theta_{21}} H_{s-n}^{(1)}(kb) \left\{ f_s s^2 J_s(ka_1) - [s J_s(ka_1) - ka_1 J_{s+1}(ka_1)] \right\}$$

$$\begin{aligned}
 & + f_0 C_s [sJ_s(k_c a_1) - k_c a_1 J_{s+1}(k_c a_1)] \\
 & = i^s \{ [sJ_s(ka_1) - ka_1 J_{s+1}(ka_1)] - f_s s^2 J_s(ka_1) \} e^{-is\theta_0}
 \end{aligned} \tag{18}$$

$$\sum_{n=-\infty}^{\infty} A_n e^{i(s-n)\theta_{12}} H_{s-n}^{(1)}(kb) J_s(ka_2) + B_s H_s^{(1)}(ka_2) - D_s J_s(k_c a_2) = -i^s J_s(ka_2) e^{-is\theta_0}, \tag{19}$$

$$\begin{aligned}
 & \sum_{n=-\infty}^{\infty} A_n e^{i(s-n)\theta_{12}} H_{s-n}^{(1)}(kb) \{ f_s s^2 J_s(ka_2) - [sJ_s(ka_2) - ka_2 J_{s+1}(ka_2)] \} \\
 & + B_s \{ f_s s^2 H_s^{(1)}(ka_2) - [sH_s^{(1)}(ka_2) - ka_2 H_{s+1}^{(1)}(ka_2)] \} \\
 & + f_0 D_s [sJ_s(k_c a_2) - k_c a_2 J_{s+1}(k_c a_2)] \\
 & = i^s \{ [sJ_s(ka_2) - ka_2 J_{s+1}(ka_2)] - f_s s^2 J_s(ka_2) \} e^{-is\theta_0}
 \end{aligned} \tag{20}$$

where $f_s = \mu_s / \mu_m$, and $f_0 = \mu_0 / \mu_m$.

Due to the mismatch of material properties across the interface between the nano-inhomogeneities and the matrix, stress concentration may exist around the nano-inhomogeneities, which may cause the damage and evolution of defects in the material. Therefore, it is of interest to examine the relations between the stress concentration and material properties of nano composites.

The dynamic stress concentration factor (*DSCF*) around the circular nano-inhomogeneity is expressed as

$$DSCF = \left| \frac{\tau_{\theta z q}^M}{\tau_0^M} \right|, \quad (q = 1, 2) \tag{21}$$

where $\tau_0^M = \mu_m W_0 k$ denotes the maximum dynamic stress resulting from the incident waves.

6 Numerical examples and analyses

In the following numerical analysis, it is convenient to make the variables dimensionless. To this end, a characteristic length a_1 , where a_1 is the radius of the nano-inhomogeneity 1, is introduced. The following dimensionless variables and quantities have been chosen for computation: the incident wave number is $k^* = ka_1 = 0.01 - 2.0$, the radius ratio of the two nano-inhomogeneities is $a^* =$

$a_2/a_1 = 0.1 - 5.0$, the distance between the two nano-inhomogeneities is $b^* = b/a_1 = 2.1 - 8.0$, the shear modulus ratio of the nano-inhomogeneity and the matrix is $f_0 = \mu_0/\mu_m = 0.1 - 10$, the shear modulus ratio of the nano-inhomogeneity and the matrix is $f_s = \mu_s/\mu_m = 0.1 - 10$, and the density ratio is $\rho = \rho_0/\rho_m = 1.0 - 3.0$.

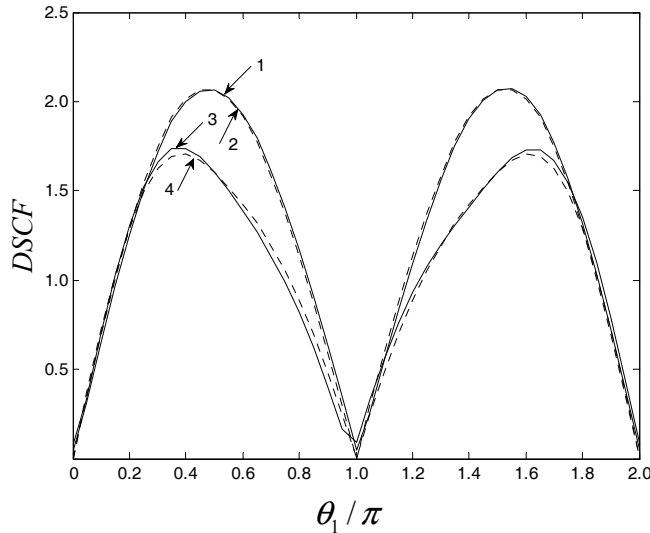


Figure 2: Comparison with the existing solutions $f_s = 0, f_0 = 0, b^* = 8, \theta_0 = 0, \theta_{21} = \pi/2$ 1 $k^* = 0.5$ obtained from this paper; 2 $k^* = 0.5$ in Pao and Mow (1973). 3 $k^* = 1.0$ obtained from this paper; 4 $k^* = 1.0$ in Pao and Mow (1973).

In order to validate the presented dynamical model, comparison with the previous literatures is given. Fig.2 shows the angular distribution of the dynamic stress around the nano-inhomogeneity with parameters: $b^* = 8.0, f_0 = f_s = 0$. If $b^* = 8.0$, the mutual interaction between the two nano-inhomogeneities disappears. When $f_0 = 0$, the inhomogeneities become holes. $f_s = 0$ means that the interface effect is ignored. The good agreements can be found in Fig.2. It can be seen that if $k^* = 0.5$, the angular distribution of DSCFs is symmetric about the two axes, and the maximum dynamic stress occurs at the position of $\theta = \pi/2$. In the case of high frequency ($k^* = 1.0$), the maximum dynamic stress has a trend of shifting towards the shadow side of the hole. The above conclusion is consistent with that in Pao and Mow (1975).

Fig. 3 illustrates the distribution of the dynamic stress around the nano-inhomogeneity 1 with different values of f_s when the center-to-center distance is large. Through comparison, it can be found that when the interface effect is considered, the dy-

dynamic stress at the positions near $\theta_1 = \pi/2$ and $\theta_1 = 3\pi/2$ decreases greatly with the increase of f_s . The kind of trends means that if the value of f_s is large enough, the dynamic stress concentration along the nano-inhomogeneity 1 will vanish.

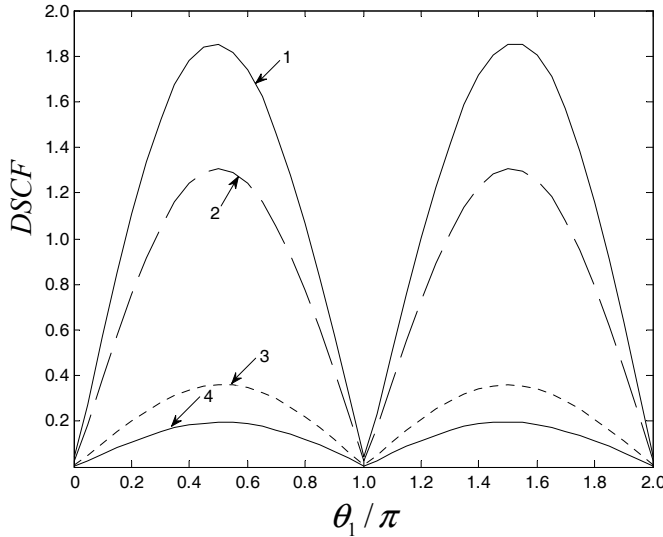


Figure 3: Dynamic stress distribution around the nano-inhomogeneity 1 with $k^* = 0.5, f_0 = 0, b^* = 8, \theta_{21} = \pi/2, \theta_0 = 0$ 1. $f_s = 0.1$; 2. $f_s = 0.5$; 3. $f_s = 4.0$; 4. $f_s = 8.0$.

In the region of low frequency with $k^* = 0.5$, the distribution of the dynamic stress around the nano-inhomogeneity 1 with different values of f_s is shown in Fig. 4. For a small separation of $b^* = 2.5$, the interaction between the two nano-inhomogeneities is significant. It can be seen that the *DSCF* is no longer symmetric with respect to $\theta_1 = \pi$, and the maximum dynamic stress occurs at the position near the nano-inhomogeneity 2. With the increase of f_s , the dynamic stress decreases considerably, especially at the position near the nano-inhomogeneity 2.

To find the surface/interface effect on the dynamic stress in the region of low frequency with different values of f_s , Figs. 5 and 6 are given. Fig. 5 shows the distribution of the dynamic stress around the nano-inhomogeneity 1 when the nano-inhomogeneities are stiffer than the matrix. In this case, it is clear that the value of dynamic stress declines greatly. When the interface is stiffer than the nano-inhomogeneity and matrix, the variation of dynamic stress is sensitive. However, the interface effect on the dynamic stress is little if the interface is soft. Fig. 6 shows the distribution of the dynamic stress around the nano-inhomogeneity 1 when the

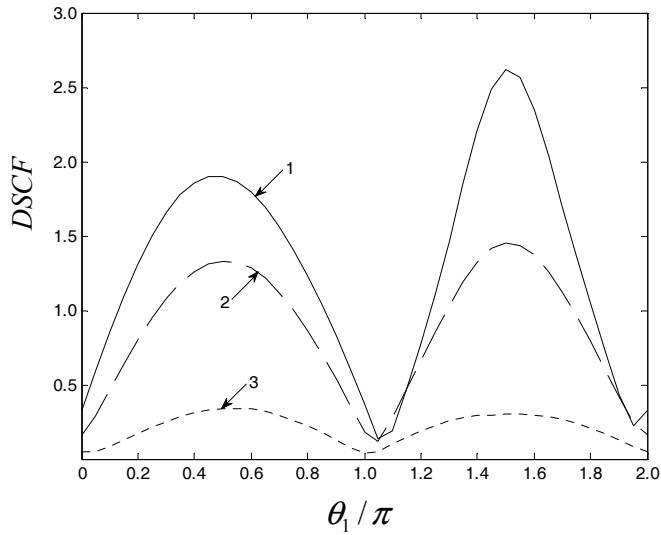


Figure 4: Dynamic stress distribution around the nano-inhomogeneity 1 with $k^* = 0.5$, $f_0 = 0$, $b^* = 2.5$, $\theta_{21} = \pi/2$, $\theta_0 = 0$ 1. $f_s = 0.1$; 2. $f_s = 0.5$; 3. $f_s = 4.0$.

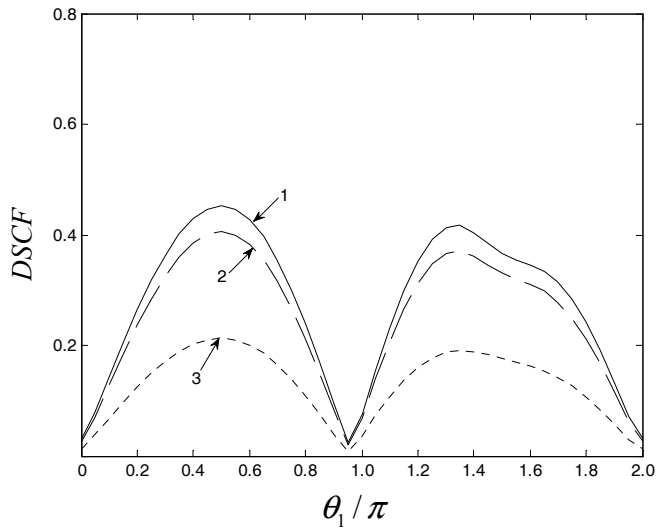


Figure 5: Dynamic stress distribution around the nano-inhomogeneity 1 with $k^* = 0.5$, $f_0 = 3.0$, $b^* = 2.5$, $\theta_{21} = \pi/2$, $\theta_0 = 0$, $\rho = 2.0$ 1. $f_s = 0.1$; 2. $f_s = 0.5$; 3. $f_s = 4.0$.

nano-inhomogeneities are softer than the matrix. It can be observed that due to a small shear modulus ratio f_0 , the effect of nano-inhomogeneity on the dynamic stress is insensitive. Comparing with the results in Figs. 5 and 6, it can be also found that the interface effect increases if the nano-inhomogeneity is softer.

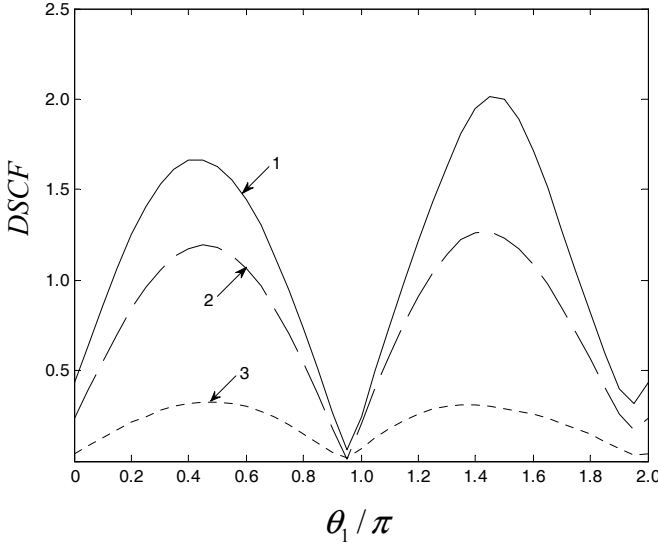


Figure 6: Dynamic stress distribution around the nano-inhomogeneity 1 with $k^* = 0.5, f_0 = 0.3, b^* = 2.5, \theta_{21} = \pi/2, \theta_0 = 0, \rho = 2.0$ 1. $f_s = 0.1$; 2. $f_s = 0.5$; 3. $f_s = 4.0$.

For a high frequency of $k^* = 1.5$, Fig.7 displays the distribution of the dynamic stress around the nano-inhomogeneity 1 when the nano-inhomogeneities are stiffer than the matrix. In the case with different values of f_s , the maximum $DSCF$ appears at the positions of $\theta_1 = 0.6\pi$ and $\theta_1 = 1.4\pi$. Compared with the results in Fig.5, it can be seen that with the increase of wave frequency, the maximum dynamic stress increases if the interface is softer. However, if the interface is stiffer, the variation of the maximum dynamic stress is very little. It can be also found that the value of $DSCF$ near $\theta_1 = \pi$ increases slightly.

Fig.8 illustrates the effect of the relative position of the two nano-inhomogeneities on the dynamic stress around the nano-inhomogeneity 1 with parameters: $k^* = 0.5, f_0 = 3.0, f_s = 0.1, b^* = 2.5$. One can see that the distribution of the maximum $DSCF$ shows great variation with the relative position of the two nano-inhomogeneities, especially at the illuminate sides of nano-inhomogeneity. When the relative position of the two nano-inhomogeneities varies, the $DSCF$ at the po-

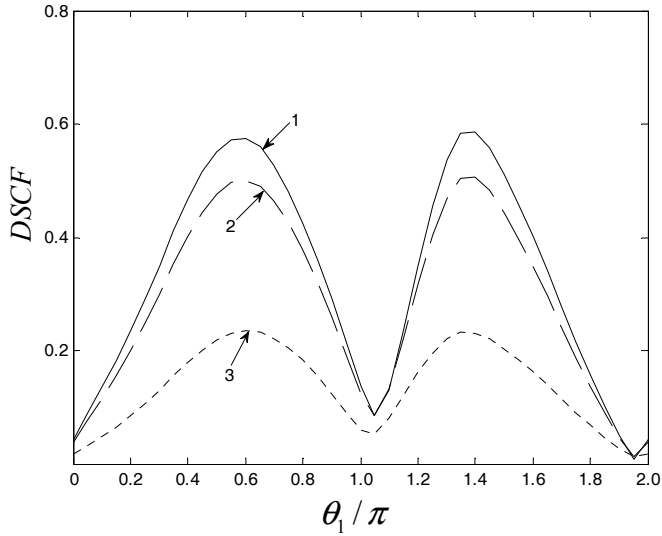


Figure 7: Dynamic stress distribution around the nano-inhomogeneity 1 with $k^* = 1.5, f_0 = 3.0, b^* = 2.5, \theta_{21} = \pi/2, \theta_0 = 0, \rho = 2.0$ 1. $f_s = 0.1$; 2. $f_s = 0.5$; 3. $f_s = 4.0$.

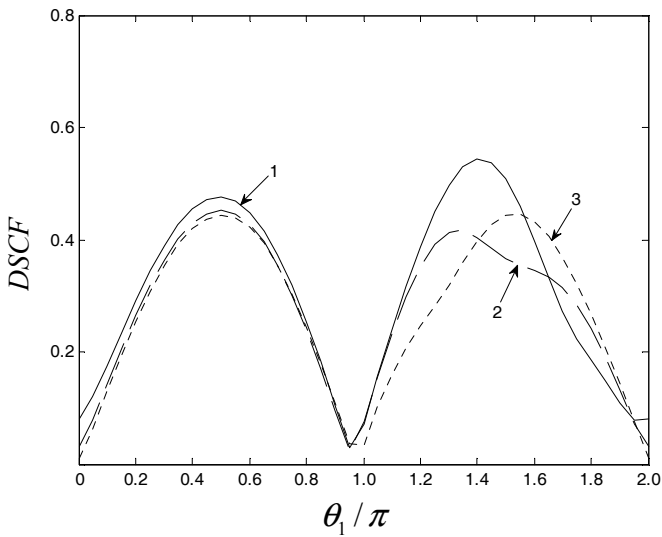


Figure 8: Dynamic stress distribution around the nano-inhomogeneity 1 with $k^* = 0.5, f_0 = 3.0, f_s = 0.1, b^* = 2.5, \theta_0 = 0, \rho = 2.0$ 1. $\theta_{21} = \pi/3$; 2. $\theta_{21} = \pi/2$; 3. $\theta_{21} = 2\pi/3$.

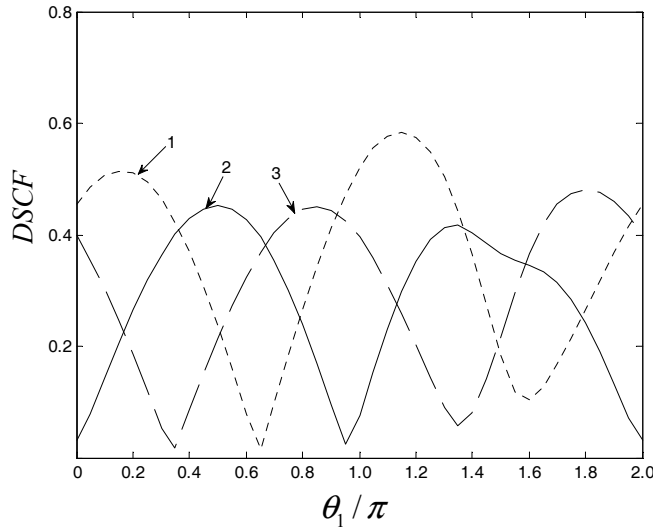


Figure 9: Dynamic stress distribution around the nano-inhomogeneity 1 with $k^* = 0.5, f_0 = 3.0, f_s = 0.1, b^* = 2.5, \theta_{21} = \pi/2, \rho = 2.0$. 1. $\theta_0 = 0$; 2. $\theta_0 = \pi/3$; 3. $\theta_0 = -\pi/3$.

sitions near the nano-inhomogeneity 2 varies considerably, while it expresses no variation at the position of $\theta_1 = \pi/2$. So, it can be concluded that the relative position of the two nano-inhomogeneities shows great effect on the dynamic stress when they are too close. The interface effect also increases when the two nano-inhomogeneities are close.

To illustrate the effect of the incident angle on the dynamic stress around the nano-inhomogeneity 1, Fig.9 is given. It can be seen when the incident angle is different, the position of the maximum dynamic stress shows great variation. With the increase of the incident angle, the maximum dynamic stress increases obviously. At the illuminate sides of nano-inhomogeneity, the variation of the maximum dynamic stress with the incident angle is greater.

7 Conclusion

In this paper, the interaction between the two nano-inhomogeneities subjected to anti-plane shear waves is studied. The model of Gurtin and Murdoch Gurtin's has been adopted to analyze the interface effect. The wave fields are expressed by wave function expand method, and the addition theorem is used to accomplish the superposition of wave fields. Comparison with the previous investigations validates

this presented model. Through analyzing the interface effect on the dynamic stress in nano composites, the methods of reducing the dynamic stress and increasing the strength of nanosized structures are found. The main findings of this work are as follows.

(1) The dynamic stress decreases with the increase of f_s . When the value of f_s is > 1.0 , the maximum dynamic stress becomes very little. With the increase of f_s , the value of $DSCF$ decreases continuously almost in the whole range.

(2) If the nano-inhomogeneities are stiffer than the matrix, the dynamic stress around the nano-inhomogeneity is little. When the interface is stiffer than the nano-inhomogeneity and matrix, the variation of dynamic stress is considerable.

(3) Due to the softer interface, the maximum $DSCF$ increases with the increase of wave frequency.

However, when the interface is stiffer, the variation of the maximum $DSCF$ is very little.

(4) For a small separation, the interaction between the nano-inhomogeneities is fairly strong, and the surface/interface effect increases great. The relative position of the two nano-inhomogeneities also shows great effect on the dynamic stress around the nano-inhomogeneities.

(5) The dynamic stress at the shadow sides increases with the increase of the incident angle.

These finding can provide reference of significant reference for the design and analysis of nano composites. The solving method in this study can also be extended to the cases of three or more interacting nanoinhomogeneities.

Acknowledgement: The paper is supported by the National Natural Science Foundation of China (Foundation No. 10972147), the Natural Science Foundation of Hebei Province, China (Foundation No. A2010001052), the specialized scientific research fund projects for postgraduate in Shijiazhuang Tiedao University, and the Program No. IRT0971 for Changjiang Scholars and Innovative Research Team in University.

References

- Cahn, J. W.; Larché, F.** (1982): Surface stress and chemical equilibrium of small crystals—II. Solid particles embedded in a solid matrix. *Acta Metallurgica*, vol. 30, pp. 51–56.
- Cammarata, R. C.** (1994): Surface and interface stress effects in thin films. *Progress in Surface Science*, vol. 46, pp. 1–38.

Cheng, H.C.; Hsu, Y.C.; Chen, W.H. (2009): The influence of structural defect on mechanical properties and fracture behaviors of carbon nanotubes. *CMC: Computers, Materials & Continua*, vol. 11, pp. 127–146.

Duan, H. L.; Wang, J.; Huang, Z. P.; Karihaloo, B. L. (2005): Size-dependent effective elastic constants of solids containing nanoinhomogeneities with interface stress. *Journal of the Mechanics and Physics of Solids*, vol. 53, pp. 1574–1596.

Fang, X. Q.; Zhang, L. L.; Wang, X. H. (2010): Interface effect on the dynamic stress around an elliptical nano-Inhomogeneity subjected to anti-plane shear waves. *CMC: Computers, Materials & Continua*, vol. 16, pp. 229–246.

Gurtin, M. E.; Murdoch, A. I. (1975): A continuum theory of elastic material surfaces. *Archives of Rational Mechanics and Analysis*, vol. 57, pp. 291–323.

Gurtin, M. E.; Weissmüller, J.; Larché, F. (1998): A general theory of curved deformable interfaces in solids at equilibrium. *Philosophical Magazine A*, vol. 78, pp. 1093–1109.

Li, Z. R.; Lim, C. W.; He, L. H. (2005): Stress concentration around a nano-scale spherical cavity in elastic media: effect of surface stress. *European Journal of Mechanics A/Solids*, vol. 25, pp. 260–270.

Nix, W. D.; Gao, H. (1998): An atomistic interpretation of interface stress. *Scripta Materialia*, vol. 39, pp. 1653–1661.

Pao, Y. H.; Mow, C. C. (1973): *Diffraction of elastic waves and dynamic stress concentration*. Crane-Russak, New York.

Sharma, P.; Ganti, S. (2002): Interfacial elasticity corrections to size-dependent strain-state of embedded quantum dots. *Physica Status Solidi*, vol. 234, pp. 10–12.

Sharma, P.; Ganti, S.; Bhate, N. (2003): Effect of surfaces on the size-dependent elastic state of nano-inhomogeneities. *Applied Physics Letters*, vol. 82, pp. 535–537.

Wu, X. F.; Dzenis, Y. A. (2006): Wave propagation in nanofibers. *Journal of applied physics*, vol. 100, 124318.

